RSC Advances

ROYAL SOCIETY OF CHEMISTRY

www.rsc.org/advances

Cite this: DOI: 10.1039/c0xx00000x

www.rsc.org/xxxxxx

ARTICLE TYPE

Integrated pneumatic micro-pumps for high-throughput droplet-based microfluidics†

Jae-Won Choi,[‡a] Sangmin Lee,[‡b] Dong-Hun Lee,[c] Joonwon Kim,*[b] Andrew J. deMello*[d] and Soo-Ik Chang*[a]

Received (in XXX, XXX) Xth XXXXXXXXX 20XX, Accepted Xth XXXXXXXXX 20XX
DOI: 10.1039/b000000x

Droplet-based microfluidic systems have recently emerged as powerful experimental tools in the chemical and biological sciences. In conventional droplet-based microfluidics, controlled droplet generation is normally achieved using precision syringe pumps, where sample is delivered to the microdevice using external tubing that possesses an appreciable dead volume. Accordingly, there is an unmet need for a droplet generation system that does not require the use of syringe pumps. Herein, we report the integration of pneumatic micro-pumps with droplet-based microfluidic systems and their subsequent use in high-throughput biological experimentation. The efficacy of the system is demonstrated by investigating the interaction and the binding inhibition between angiogenin and the anti-angiogenin antibody with a dissociation constant (K_D) value of 9.1±3.5 nM and a half maximal inhibitory concentration (IC_{50}) value of 12.2 ± 2.5 nM, respectively.

Introduction

Droplet-based (or segmented-flow) microfluidic systems have recently emerged as powerful experimental tools in the chemical and biological sciences.[1-4] Such systems are particularly well suited to performing high-throughput experimentation since isolated sub-nanoliter volume droplets can be formed at rates in excess of one thousand droplets per second. In addition, the chemical (or biological) payload of individual droplets can be varied at will and reagent mixing achieved on a millisecond timescale via chaotic advection.[5,6]

Not surprisingly, droplet-based microfluidic systems have been applied to a variety of biological problems[2,7] including cell-based enzymatic assays,[6] hybridoma screening,[8] cell death assays[9] and drug candidate screening.[10] In addition, a variety of detection methods for probing biological reactions within such droplets have been developed. These include time-integrated fluorescence spectroscopy,[11] fluorescence lifetime imaging (FLIM),[12] fluorescence resonance energy transfer (FRET),[13,14] fluorescence polarisation (FP),[15] mass spectrometry,[16] and surface enhanced Raman scattering (SERS).[17] Of particular relevance to bioanalytical measurements is FP since it is a homogenous technique that does not require the discrimination of bound and free species in the analytical sample prior to analysis.

In conventional droplet-based microfluidics, precise droplet generation is normally achieved using precision syringe pumps, where sample is delivered to the microdevice from pre-loaded syringes using external tubing possessing an appreciable dead volume. Accordingly, there is an unmet need for a droplet generation modules that do not require the use of syringe pumps. A variety of new approaches based on electrowetting,[18] droplet dispensing[19] and micro-pumps[20,21] have been developed. However, to date dispensers and micro-pumps have not been *fully* integrated with droplet-based microfluidic systems. In addition, the dispensers and micro-pumps have not been used for their application in high-throughput biological experimentation but for simple manipulation of droplets. For example, micro-droplets were generated using micro-pumps but the systems cannot be used as a microfluidic chip for bioanalysis since the droplets were generated at an off-chip without oil flow.[20,21] Recently, integrated pneumatic micro-pumps with droplet-based microfluidics were reported but still have dead volume of samples because the system is required a syringe pump to deliver oil phase into the channel.[22-24] In addition, a complex computer program for repetitive actuation of polydimethylsiloxane (PDMS) membrane at millisecond level is needed to generate microdroplets with high monodispersity. Finally, it has highly complex fabrication procedure since they used four layers (three glass layers including patterned glass and PDMS membrane) for construction of microfluidic chip.[24]

Herein, we describe the first *fully* integrated pneumatic micro-pumps with droplet-based microfluidics (i.e. without using any syringe pumps) and their subsequent use in high-throughput biological experimentation. Specifically, pneumatic micro-pumps were integrated with droplet-based microfluidics by attaching all liquid chambers to microfluidic inlet, and the fabrication procedures were simplified by using three layers of PDMS membrane (without glass etching). In addition, droplet generation can be achieved by only single step negative (suction in liquid chamber) and positive pressure (sample flow in microfluidic channel) actuation. The efficacy of the system is demonstrated by investigating the interaction and the binding inhibition between

angiogenin and the anti-angiogenin antibody. Angiogenin is a potent blood vessel inducing 14 kDa protein implicated in tumor growth and metastasis.[25]

Experimental

Materials

Phosphate-buffered saline (PBS) tablets were purchased from Amresco (Solon, OH, USA). Bovine serum albumin (BSA) was purchased from GenDEPOT (Barker, TX, USA). Mineral oil was purchased from Sigma-Aldrich (St. Louis, MO, USA). ABIL EM 90 surfactant was purchased from Evonik Industries (Essen, Germany). Polydimethylsiloxane (PDMS, Sylgard 184 silicone elastomer kit) was purchased from Dow Corning (Midland, MI, USA). Alexa Fluor 488 (AF488) protein labelling kit was purchased from Invitrogen (Carlsbad, CA, USA). Rosetta strain Escherichia coli (DE3)pLysS (carrying the angiogenin plasmid) were used for the expression of angiogenin (ANG). ANG was isolated and purified as described previously.[15]The anti-angiogenin antibody (anti-ANG Ab) was purified from rabbit serum as previously described.[26]

Preparation of standard solutions

For all experiments, 0.1 mg/ml BSA in PBS (pH 7.4) was used to dilute ANG and anti-ANG Ab. This buffer was filtered using a 0.2µm single-use syringe filter from Sartorius (Goettingen, Germany). Angiogenin was labelled using AF488 protein labelling kit according to manufacturer's protocol, and the molar ratio of dye to protein was measured using a NanoDrop 2000 spectrophotometer from Thermo Scientific (Wilmington, DE, USA). The continuous phase used in all experiments consisted of 2 % (w/w) ABIL EM 90 in mineral oil.

Fabrication of microfluidic devices

The microfluidic device is composed of three layers (a structured PDMS layer, glass and a PDMS membrane) and is clamped between a customized mount to operate the flexible membrane. Microchannels in PDMS are formed by standard soft lithographic techniques.[27,28] After soft lithographic processing, access conduits in the glass substrate were formed using a MAXNC glass-drilling machine (Gilbert, AZ, USA). The flexible membrane is made of PDMS and prepared on a flat Teflon-coated substrate. Since the Teflon-coated surface provides low adhesion to the PDMS membrane, the membrane can be easily detached from the surface and transferred to an alternate surface. Briefly, a 10:1 (weight ratio) mixture of PDMS pre-polymer and curing agent were spin coated at 750 rpm for 50 s on a flat Teflon-coated substrate. The substrate was then cured on a hot-plate at 90°C for 15 min to form a 70µm thick PDMS membrane. The bump structure was made of a polyurethane tube having outer diameter 2 mm from SMC Co. (Noblesville, IN, USA). This structure was constructed after bonding process of PDMS layers (structured and membrane) and glass substrate. Then tube is inserted in a pre-punched hole at the center of the liquid chamber of the structured PDMS layer and end of polyurethane tube is reached at the PDMS membrane. The fabrication procedure of microfluidic chip was described in supporting information (see Fig. S1, ESI†).

Detection system

The detection system for fluorescence polarisation (FP) measurements consists of a 488 nm, 10 mW diode laser (World Star Tech, Canada), an Olympus IX71 inverted fluorescence microscope (Tokyo, Japan), and dual filter system. An electron multiplying-charged coupled device from Princeton Instruments (ProEM, Trenton, NJ, USA) was used for detection of

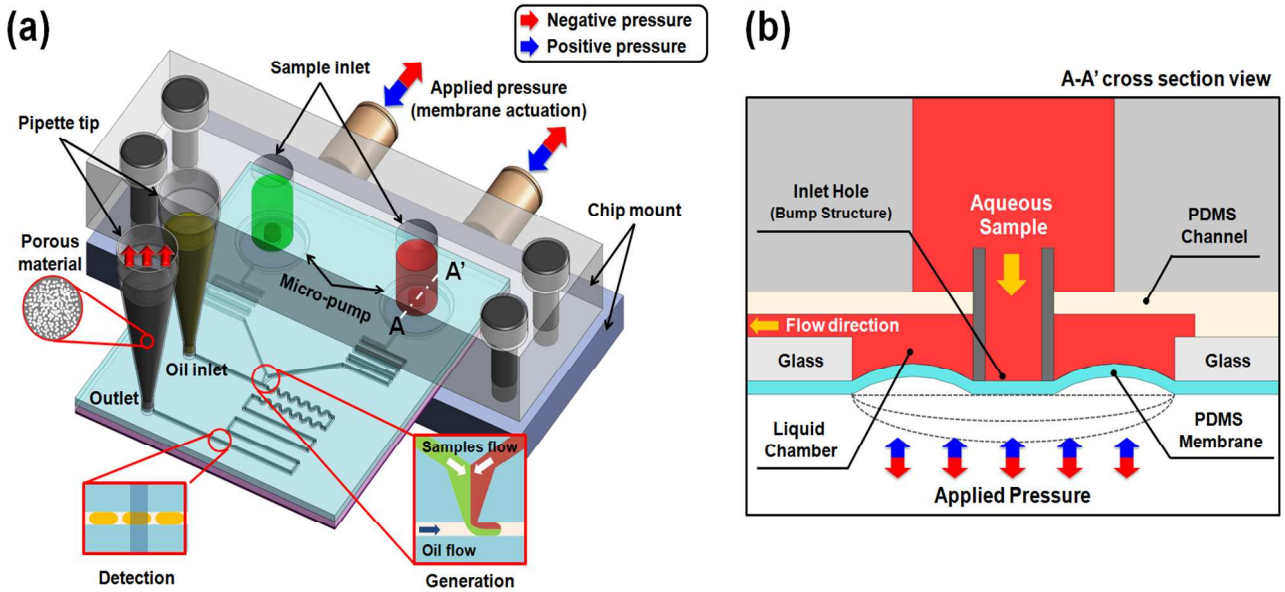

Fig. 1 (a) Schematic illustration of a droplet-based microfluidic system containing integrated pneumatic micro-pumps. (b) Cross sectional view of A-A' in part (a). The microfluidic device comprises three layers: a flexible polydimethylsiloxane (PDMS) membrane, a planar glass substrate and a micro-patterned PDMS substrate. Using polyurethane tube, bump structure is induced on the micro-patterned PDMS substrate.

Cite this: DOI: 10.1039/c0xx00000x

www.rsc.org/xxxxxx

ARTICLE TYPE

fluorescence emission. The laser beam was introduced into the microscope using beam-steering optics and then reflected by a dichroic mirror from Semrock(FF506-Di02, Rochester, NY, USA) into an 20X objective (UPLFLN20X, Olympus). Polarised emission was collected using the same objective and spectrally filtered from the excitation using the filter cube. All the optical readouts are performed on the last line of the channel (near outlet). All fluorescence data were collected using the WinSpec/32 program (Princeton Instruments) and analysed using in house software.

Results and discussion

Integrated pneumatic micro-pumps with droplet-based microfluidic system and detection system

A schematic of the integrated pneumatic micro-pump with droplet-based microfluidic system is shown in Fig. 1a. The micro-pumps consist of a liquid chamber, inlet hole with integrated "bump structure" and a flexible PDMS membrane as shown in Fig. 1b. A recess in the top PDMS channel is mated with a pre-drilled hole of the glass substrate to allow coupling. A specific image about the part of integrated microfluidic device is shown in supporting information (see Fig.S2, ESI†).

In order to generate droplets, separate micro-pumps were used to deliver the aqueous and oil phases to a microchannel T-junction. Each micro-pump membrane is controlled using a dedicated (in-house) pressure controller (homemade type) with a uniform positive pressure (<10 kPa) being applied to the membrane. Specifically, each micro-pump membrane can be actuated by applying single step negative and positive pressures with air pumps, digital regulators, pressure monitors and a solenoid valve (see Fig.S3, ESI†). The membrane pushes liquid within the microfluidic channel whilst simultaneously closing each inlet hole (see Fig. 1b). Meanwhile, oil flows into the microfluidic channel using a negative pressure applied to the outlet. A porous material (in our case cotton) is stacked in the outlet tubing adaptor to prevent the formation of an air layer (see Fig. 1a). The united sample flows then segment into droplets at the T-junction. Using this approach, subnanoliter microdroplets can be generated with ease.

Fig. 2a demonstrates that the pump is effective at generating a uniform segmented flow. Specifically, the image illustrates the formation of droplets at the T-junction with a 1:1 volume ratio of inputs at junction. Droplet size (or volume) can be controlled by varying the positive pressure (under below ~ 10 kPa) applied to the membrane, and the droplet generation frequency controlled by the negative pressure of -40 ~ -70 kPa. More specifically, we demonstrated the generation frequency of microdroplets as variation of negative pressure using pneumatic micro-pumps in Fig. 2b. For current purposes, a constant negative pressure and

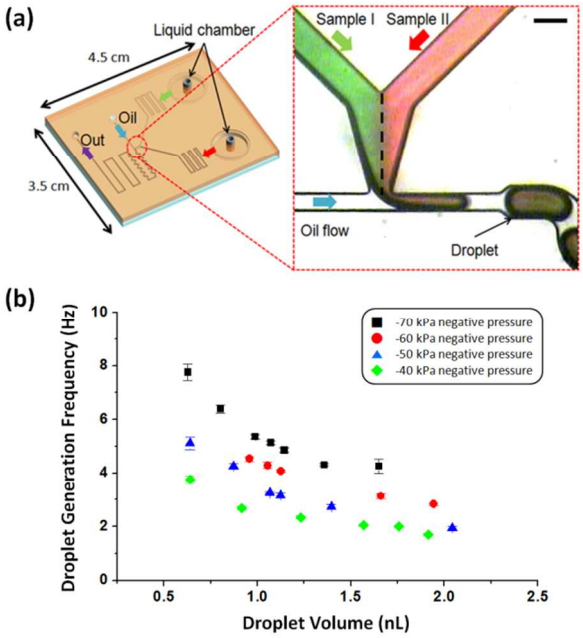

Fig. 2 (a) Schematic of the microfluidic chip and optical image of droplets generated by pneumatic micro-pumps. Volume ratio 1:1 of two sample flows is constantly maintained, schematic of the microfluidic image (left) and optical image of droplets generated with T-junction geometry (right image) using green and red food dye. In this case, droplets are generated with size of 970 pL. And positive pressure was maintained less than 10 kPa and negative pressure was maintained -70 kPa. Scale bar: 100 μm. (b) characterized droplet generation frequency and size against variation of pressure. The generation frequency and size of droplets can be controlled by varying positive and negative pressure. Also, each data shows the uniformity of the generated droplets under stable pressures.

uniform volume ratio between the two samples ensures stable droplet generation. Generated droplets have uniformity under constant pressure condition (see Fig.S4, ESI†).

Fig. 3 shows a schematic of the dual fluorescence polarisation (FP) detection system used to assay droplets in high-throughput. This detection system has recently been shown to be successful in assaying protein-protein interactions within pL-volume droplets.[15]

Analysis of binding between ANG and anti-ANG Ab

To demonstrate the efficacy of the integrated system for performing high-throughput biological assays, we firstly investigated the binding between angiogenin (ANG) and anti-angiogenin antibody (anti-ANG Ab). ANG was labelled with Alexa Fluor 488 (AF488-ANG) and the anti-ANG Ab being unlabelled.

The AF488-ANG solution was loaded via the left sample inlet, and anti-ANG Ab solution loaded via the right sample inlet as shown in Fig.1a. The loaded samples are then drawn into each liquid chamber by applying negative pressure to the flexible

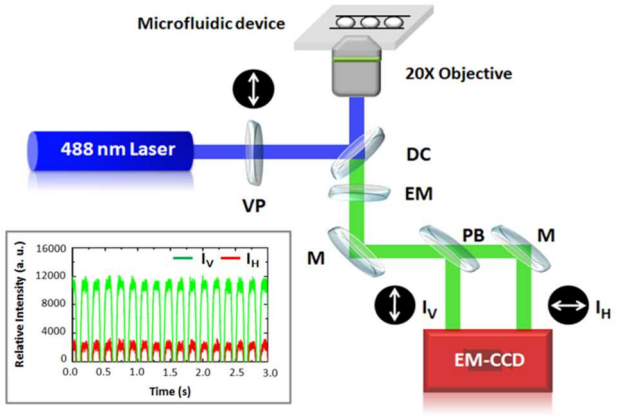

Fig. 3 Schematic of dual fluorescence polarisation detection system for analysis of biological reactions in microdroplets. I_V and I_H define the vertical intensity and horizontal intensity of the emission light, respectively. VP, vertical polariser; DC, dichroic mirror; EM, emission filter; M, mirror; PB, polarising beam splitter. The inset image shows an exemplar fluorescence signals burst scan over a period 3 seconds. The concentration of AF488-ANG is 10 nM, whilst the anti-ANG Ab concentration is 100 nM. Green lines represent I_V and red lines represent I_H.

membrane. For the binding experiments described, the concentration of anti-ANG Ab was varied from 0 to 200 nM against a fixed (final) concentration of 10 nM AF488-ANG. Droplets had a volume of 970 ± 18pL and were generated at a frequency of 5 Hz.

The inset in Fig. 3 illustrates typical I_V and I_H fluorescence burst scans over a time period of 3.0 s. I_V and I_H define the vertical emission and horizontal emission intensities, respectively. Polarisation (P) values are calculated from I_V and I_H using,

$$P = \frac{(I_V - I_H)}{(I_V + I_H)} \quad (1)$$

The variation in polarisation as a function of anti-ANG Ab concentration is presented in Fig. 4, where the increase in polarisation is due to the interaction (binding) between AF488-ANG and anti-ANG Ab. When a small fluorescent molecule is excited with polarised light, the emitted light is largely depolarised because molecules rotate rapidly in solution. However, if the small fluorescent molecule is bound by a larger molecule such as antibody, the emitted light is largely polarised because its effective molecular volume will be increased.[15] A nonlinear least-squares fit of the data to equation (2) yields a K_D value of 9.1±3.5 nM.

$$P = P_{min} + \Delta P \left(\frac{[anti\text{-}ANG\ Ab]}{K_D + [anti\text{-}ANG\ Ab]}\right) \quad (2)$$

Here P is the measured polarisation, P_{min} is the polarisation of the unbound AF488-ANG, ΔP is total change in polarisation, and $[anti\text{-}ANG\ Ab]$ is total concentration of anti-ANG Ab. The extracted K_D value is in good agreement with previously reported values of 16.6 ± 2.4 nM and 10.4 ± 3.3 nM from droplet-based experiments incorporating syringe pumps and either FRET or FP detection, respectively. [13,15]

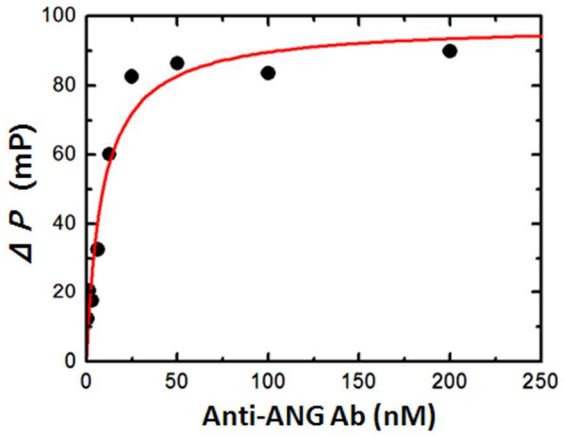

Fig. 4. Extracted binding curve between AF488-ANG and anti-ANG Ab. The concentration of AF488-ANG was fixed at 10 nM, and anti-ANG Ab concentration was varied from 0 to 200 nM.

Analysis of binding inhibition between AF488-ANG and anti-ANG Ab by unlabelled ANG

Next, to extend our experimental approach to high-throughput inhibitor screening applications, the inhibition of the interaction between AF488-ANG and anti-ANG Ab by unlabelled ANG was assayed. It is noted that unlabelled ANG is a competitive inhibitor for the AF488-ANG/ANG-Ab interaction. Mixtures of AF488-ANG and unlabelled ANG were loaded via the left sample inlet, and solutions of anti-ANG Ab were loaded via the right sample inlet as shown in Fig.2a. In this experiment, the final concentration of unlabelled ANG was varied from 0 to 800 nM against a fixed final concentration of 10 nM of AF488-ANG and 20 nM anti-ANG Ab. Fig.5 illustrates the analysis of binding

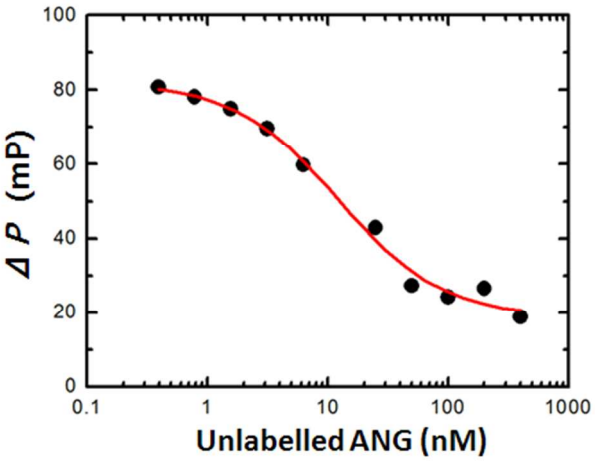

Fig. 5 Inhibition of the binding between AF488-ANG and anti-ANG Ab by unlabelled ANG. The concentration of unlabelled ANG was varied from 0 to 800 nM against a fixed concentration of 10 nM of AF488-ANG and 20 nM anti-ANG Ab.

inhibition between AF488-ANG and anti-ANG Ab by unlabelled ANG. A nonlinear least-squares fit of the data to the model defined in equation (3) yields a half maximal inhibitory

concentration (IC_{50}) value of 12.2 ± 2.5 nM, P_{min}= 18.8 ± 3.4 mP and P_{max}= 80.8 ± 3.0 mP.

$$P = P_{min} + \frac{(P_{max} - P_{min})}{(1+ 10^{([UnlabelledANG]-\mathrm{LogIC50})}} \quad (3)$$

Conclusion

We have developed the integration of pneumatic micro-pumps with droplet-based microfluidic systems for high-throughput biological experimentation. Importantly, the total footprint of the droplet-based analysis system is significantly reduced when compared to conventional systems that incorporate syringe pumps for fluid motivation. In typical syringe pump-based microfluidic systems, two or three aqueous inlets and one oil-inlet are used to establish interaction and binding inhibition experiments. Accordingly, three or four syringes pumps are required to control individual inlet. Through the use of pneumatic micro-pumps, a single pressure controller can apply both negative and positive pressures to the flexible PDMS membrane and achieve fluid motivation.

In conclusion, we have successfully demonstrated the fabrication and operation of a droplet-based microfluidic system containing integrated pneumatic micro-pumps. The microfluidic device is able to perform high efficiency and high-throughput analysis of protein-protein interactions in segmented flows. To this end, we expect that the integrated microdevice is ideally suited for high-throughput screening of therapeutic antibodies, aptamers and inhibitors against specific targets.

Acknowledgements

This work was supported by National Research Foundation of Korea (NRF) grant funded by the Ministry of Science, ICT & Future Planning (MSIP) of Korea (Grant Numbers K20904000004-13A0500-00410 and 2011-0030075).

Notes and references

[a]*Department of Biochemistry, Chungbuk National University, Cheongju 361-763, Republic of Korea. Fax: +82-43-267-2306; Tel:+82-43-261-2318; E-mail: sichang@chungbuk.ac.kr*
[b]*Department of Mechanical Engineering, Pohang University of Science and Technology, Pohang 790-784, Republic of Korea. Fax:+82-54-279-5899; Tel: +82-54-279-2185; E-mail: joonwon@postech.ac.kr*
[c]*Department of Microbiology, Chungbuk National University, Cheongju 361-763, Republic of Korea.*
[d]*Department of Chemistry and Applied Biosciences, ETH Zürich, Zürich CH-8093, Switzerland.Tel: +41-44-633-66-10; E-mail: andrew.demello@chem.ethz.ch*

† Electronic Supplementary Information (ESI) available: The specific images and fabrication procedure about the part of integrated microfluidic device. See DOI: 10.1039/b000000x/

‡ These authors contributed equally to this work.

1 G. M. Whitesides, *Nature*, 2006, **442**, 368-373.
2 C. E. Stanley, R. C. Wootton, A. J. deMello,*Chimia*, 2012, **66**, 88-98.
3 S. Cho,D. K. Kang, J. Choo, A. J. deMello, S. I. Chang, *BMB Rep*., 2011, **44**, 705-712.
4 A. B. Theberge, F. Courtois, Y. Schaerli, M. Fischlechner, C. Abell, F. Hollfelder, W. T. Huck, *Angew. Chem., Int. Ed.*, 2010, **49**, 5846-5868.
5 H. Song, D. L. Chen, R. F. Ismagilov, *Angew. Chem., Int. Ed.*, 2006, **45**, 7336-7356.
6 A. Huebner, L. F. Olguin, D. Bratton, G. Whyte, W. T. Huck, A. J. deMello, J. B. Edel, C. Abell, F. Hollfelder, *Anal. Chem.*,2008, **80**, 3890-3896.
7 V. Taly, D. Pekin, A. El Abed, P. Laurent-Puig, *Trends Mol. Med.*, 2012,**18**, 405-416.
8 B. El Debs, R. Utharala, I. V. Balyasnikova, A. D. Griffiths, C. A. Merten, *Proc. Natl. Acad. Sci. U.S.A.,* 2012, **109**, 11570-11575.
9 E. Brouzes, M. Medkova, N. Savenelli, D. Marran, M. Twardowski, J. B. Hutchison, J. M. Rothberg, D. R. Link, N. Perrimon, M. L. Samuels, *Proc. Natl. Acad. Sci.U.S.A.,* 2009,**106**, 14195-14200.
10 O. J. Miller, A. El Harrak, T. Mangeat, J. C. Baret, L. Frenz, B. El Debs, E. Mayot, M. L. Samuels, E. K. Rooney, P. Dieu,M. Galvan, D. R. Link, A. D. Griffiths, *Proc. Natl. Acad. Sci. U.S.A.*, 2012, **109**, 378-383.
11 H. Song, R. F. Ismagilov, *J. Am. Chem. Soc.*,2003, **125**, 14613-14619.
12 X. Casadevall i Solvas, M. Srisa-Art, A. J. deMello, J. B. Edel, *Anal. Chem.,* 2010, **82**, 3950-3956.
13 M. Srisa-Art, D. K. Kang, J. Hong, H. Park, R. J. Leatherbarrow, J. B. Edel, S. I. Chang, A. J. deMello, *ChemBioChem* 2009, **10**, 1605-1611.
14 X. Niu, F. Gielen, J. B. Edel, A. J. deMello, *Nat. Chem.,* 2011, **3**, 437-442.
15 J. W. Choi, D. K. Kang, H. Park, A. J. deMello, S. I. Chang, *Anal. Chem.* 2012, **84**, 3849-3854.
16 R. Tian, X. D. Hoa, J. P. Lambert, J. P. Pezacki, T. Veres, D. Figeys, *Anal. Chem.,*2011, **83**, 4095-4102.
17 H. Chon, C. Lim, S. M. Ha, Y. Ahn, E. K. Lee, S. I. Chang, G. H. Seong, J. Choo, *Anal. Chem.* 2010, **82**, 5290-5295.
18 S. K. Fan, H. Yang, W. Hsu, *Lab Chip,* 2011, **11**, 343-347.
19 J. Xu, D. J. Attinger, *Micromech. Microeng.,* 2007, **18**, 065020.
20 S. Lee, J. Kim, *Micromech. Microeng.*, 2010, **20**, 015011.
21 G. Su, P. W. Longest, R. M. Pidaparti, *Biomicrofluidics*, 2010, **4**, 044108.
22 Y. Zeng, M. Shin, T. Wang, *Lab Chip.*, 2013, **13**, 267-273.
23 S. Zeng, B. Li, X. Su, J. Qin, B. Lin, *Lab Chip*, 2009, **9**, 1340-1343.
24 X. Sun, K. Tang, R. D. Smith, R. T. Kelly, *Microfluid. Nanofluidics*, 2013, **15**, 117-126.
25 N. Yoshioka, L. Wang, K. Kishimoto, T. Tsuji, G. F. Hu,*Proc. Natl. Acad. Sci.U.S.A.,* 2006, **103**, 14519-14524.
26 S. I. Chang, G. B. Jeong, S. H. Park, B. C. Ahn, J. D. Choi, S. K. Namgong, S. I. Chung, *Biochem. Biophys. Res. Commun.,* 1997, **232**, 323−327.
27 N. P. Beard, J. B. Edel, A. J. deMello, *Electrophoresis*, 2004, **25**, 2363-2373.
28 R. Gao, N. Choi, N. S. I. Chang, S. H. Kang, J. M. Song, S. I. Cho, D. W. Lim, J. Choo, *Anal. Chim. Acta*, 2010, **681**, 87−91.

Cite this: DOI: 10.1039/c0xx00000x

www.rsc.org/xxxxxx

ARTICLE TYPE